

Phase-slip avalanches in the super flow of ^4He through arrays of nanopores

David Pekker, Roman Barankov, and Paul M. Goldbart
 Department of Physics, University of Illinois at Urbana-Champaign,
 1110 West Green Street, Urbana, Illinois 61801-3080, USA
 (Dated: June 21, 2006)

Recent experiments by Sato et al. [1] have explored the dynamics of ^4He super flow through an array of nanopores. These experiments have found that, as the temperature is lowered, phase-slippage in the pores changes its character, from synchronous to asynchronous. Inspired by these experiments, we construct a model to address the characteristics of phase-slippage in super flow through nanopore arrays. We focus on the low-temperature regime, in which the current-phase relation for a single pore is linear, and thermal fluctuations may be neglected. Our model incorporates two basic ingredients: (1) each pore has its own random value of critical velocity (due, e.g., to atomic-scale imperfections), and (2) an effective inter-pore coupling, mediated through the bulk superfluid. The inter-pore coupling tends to cause neighbours of a pore that has already phase-slipped also to phase-slip; this process may cascade, creating an avalanche of synchronously slipping phases. As the temperature is lowered, the distribution of critical velocities is expected to effectively broaden, owing to the reduction in the superfluid healing length, leading to a loss of synchronicity in phase-slippage. Furthermore, we find that competition between the strength of the disorder in the critical velocities and the strength of the inter-pore interaction leads to a phase transition between non-avalanching and avalanching regimes of phase-slippage.

PACS numbers: 67.40.-w, 67.40.Hf, 83.60.Df

Quantum phenomena at the macroscopic scale have been exhibited in a variety of physical settings, including superconductors [2], the helium superfluids [3], and, more recently, Bose-Einstein condensates (BEC) in atomic vapours [4], and perhaps even supersolids [5]. Spectacular examples include persistent currents in multiply-connected superconductors and superfluids, and the Josephson effects [6], first realised in superconducting tunnel junctions [7, 8] and, later, between two weakly coupled BECs [9], as well as in superfluid ^3He [10, 11, 12] and ^4He [13, 14] weak links.

Widely-used descriptions of these systems are based upon the unifying concept of spontaneous symmetry breaking [15], implemented within the framework of the Landau theory of phase transitions. In this framework, one introduces a suitable macroscopic Ginzburg-Landau order parameter to characterise the broken symmetry state. One major virtue of order-parameter based descriptions is the view they afford of important topological processes, such as vortex nucleation and growth, and the mechanisms for dissipation that ensue.

Superconducting macroscopic quantum phenomena (MQP) have been employed in many technologies, in fields ranging from biotechnology to radio astronomy. Primarily based on the DC Josephson effect—the essential element in superconducting quantum interference devices (SQUIDs)—these include SQUID amplifiers, metrology, biology and medicine, nondestructive testing, geomagnetism, magnetic measurements and microscopy, and prospecting for oil and minerals [16].

The superfluid analogue of the SQUID differs in an essential way from its superconducting counterpart: it is sensitive to interference amongst (charge-neutral) atoms rather than (charged) electrons. As a result, it has considerable potential for use in measuring angular veloci-

ties rather than magnetic fields and, therefore, for use as an ultra-sensitive gyroscope [17, 18]. As with SQUIDs, the essential element is the DC Josephson effect, which has been realised in ^3He [10, 11] and, more recently, in ^4He [13, 14]. The latter is expected to be more useful, technologically, owing to its relatively high operating temperature, which exceeds that of ^3He -based systems by a factor of two thousand.

Recent experiments by the Berkeley group [1] have explored a system that comprises two superfluid reservoirs coupled via an array of pores, over a wide range of temperatures [21]. It was observed that, for progressively lower temperatures below the critical temperature T_c for the transition to the superfluid state, the system passes through several regimes. Just below T_c , for sufficiently small supercurrents, the array was observed to function as a single effective Josephson junction having an essentially sinusoidal current-phase relation. For lower temperatures, below roughly a few millikelvin below T_c , it was observed that the single-pore dynamics becomes irreversible. This is due to the dissipative phase-slips that occur whenever the superflow velocity in a pore reaches a critical value [22, 23, 24, 25], which we believe to be specific to that pore. At the high-temperature end of this regime, there is a narrow interval of temperatures, of width roughly 10 mK, within which all pores appear to phase-slip simultaneously, and which Sato et al. [1] refer to as the synchronous regime. At lower temperatures, down to roughly 160 mK below T_c , it appears that simultaneity in phase-slipping is lost; Sato et al. refer to this as the asynchronous regime. It is believed that technologically viable devices can be designed to function in both the Josephson (i.e. reversible) and phase-slippage (i.e. irreversible) regimes, provided a large enough fraction of pores slip sufficiently simultaneously to produce

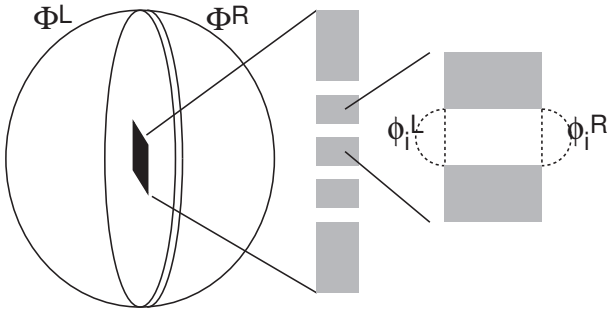


FIG. 1: Schematic of the model system. Left: the location of the pore array on the membrane is indicated by the black region, and the phases on hemispheres at infinity are labelled ϕ^L and ϕ^R . Centre: slice through the membrane, with pores being represented by breaks in the membrane (white). Right: boundary conditions on hemispheres at the openings of the i -th pore.

a measurable "whistle" at the Josephson frequency [26]. We remark that, in the setting of multi-link superconducting devices, it has been shown that the irreversible regime can be utilised for magnetic field and related phase-sensitive measurements [27].

In this Paper, we address the issue of the transition from synchronous to asynchronous phase-slip dynamics of an array of nanopores connecting a pair of superfluid reservoirs. The main ingredients of our description are pores that have random, temperature-dependent critical velocities, along with an effective inter-pore coupling mediated via superflow in the reservoirs. We develop a model that incorporates these ingredients, and analyse it via both a mean-field approximation and exact numerical analysis for arrays consisting of a relatively small number of pores. Thus, we identify two effects: (a) strong disorder washes out the synchronicity of phase slips, which leads to the loss of the "whistle"; and (b) if the disorder is sufficiently weak, the phase-slip dynamics undergoes a disorder-driven phase transition between avalanching and non-avalanching regimes (see Fig. 2). This enables us to obtain the current-phase relation, as well as the amplitude of the current oscillations at the Josephson frequency corresponding to a fixed chemical-potential difference. We believe that this model and our analysis of it captures the essential physics taking place in the Berkeley group's experiments [1].

Disparate physical systems featuring competition between quenched disorder and interactions, such as sliding tectonic plates [28], random-field magnets [29], and solids with disorder-pinned charge-density waves (CDWs) [30, 31], are well known to show phenomena analogous to the avalanching-to-non-avalanching transition described here. The model and analysis that we employ are similar to those that have been applied in the aforementioned settings [32].

Basic model | The system we wish to describe consists of two reservoirs of superfluid ^4He , separated by a rigid

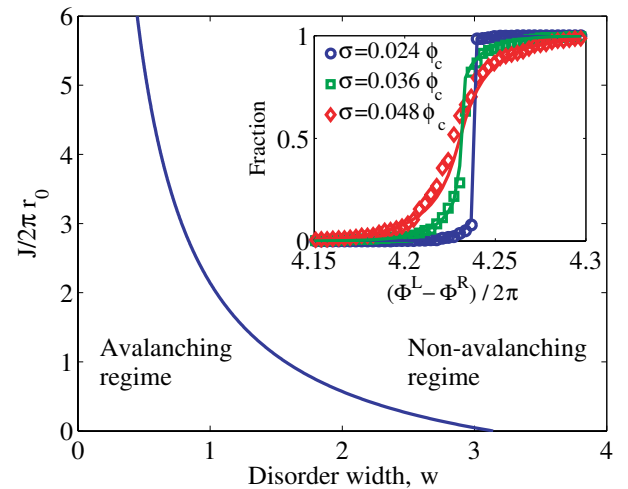


FIG. 2: Phase diagram showing avalanching and non-avalanching regimes of the phase-slip dynamics, as a function of the effective pore strength $J=2\pi r_0$ and disorder strength w . The diagram was computed via our mean-field theory, in the large-array limit, with top-hat critical phase twist (or, equivalently, the velocity) distribution of width w . Inset: The fraction of pores that have phase slipped, as a function of the control-parameter $(\phi^L - \phi^R)/2\pi$. Comparison between numerics for a 25×25 array of pores (points) and our mean-field theory (lines) with Gaussian distribution of critical velocities.

barrier, embedded in which is an array of pores, as shown in Fig. 1. We shall specialise to the case of an $N \times N$ array of pores, each having radius r_0 , situated at the sites of a square lattice of lattice parameter λ . It is straightforward to extend our analysis to other array geometries. It is convenient to regard the system as comprising three components: two are bulk components [i.e., the left (L) and right (R) reservoirs]; the third consists of the superfluid inside the pores. We describe the state of the bulk helium in terms of the superfluid order-parameter phase fields $\phi^{L/R}(\mathbf{r})$. In doing this we are neglecting effects of amplitude excitations of the order parameter, including vortices. In contrast, within the pores we retain both amplitude and phase degrees of freedom. We imagine controlling the system by specifying the two phases, $\phi^{L/R}$, to which the phases in the left and right reservoirs tend, far from the pore array. We believe that this level of description allows us to capture the following important elements: (a) pores that exhibit narrow-wire-like metastable states, these states being connected by phase slips; and (b) interactions mediated through the bulk superfluid in the two reservoirs, which couple pairs of pores to one another and also couple the pores to the control phases, $\phi^{L/R}$.

To summarise, we describe the bulk superfluid helium reservoirs by the phase-only Hamiltonians

$$H^{L/R} = \frac{K_s}{2} \int_{L/R} d^3r r^2 |\phi^{L/R}(\mathbf{r})|^2; \quad (1)$$

where $K_s = \frac{1}{2} \rho_s v_s^2$ is the superfluid stiffness, in which

n_s is the superfluid number density and m is the mass of a ^4He atom. To account for phase-slippage processes within a pore, which arise from vortex lines crossing the pore, we shall use a modified phase-only model that keeps track of the number of phase slips. Therefore, we take the energy of the superfluid inside the i^{th} pore to be

$$H_i = \frac{K_s}{2} J \left(\frac{L}{r_i} - \frac{R}{r_i} \right)^2 n_i^2; \quad (2)$$

in which $J = \frac{2}{3}d$ accounts for the geometry of the pore, where d is of the order of the membrane thickness, and $\frac{L}{r_i}$ is the phase of the order parameter in the vicinity of the left/right side of the i^{th} pore. Furthermore, n_i counts the net number of phase slips that would occur in the i^{th} pore if the system were to progress from a reference state in which the phase were uniform throughout. This description of the pores must be supplemented by specifying the critical velocities at which phase slips occur, as we shall discuss in detail below.

To reduce the model to one involving only the phase-differences across the pores and the phases at infinity, we minimize the energy (1) in the reservoirs, which forces $\frac{L}{R}$ (r) to obey the Laplace equation. Focusing on the left reservoir, the appropriate boundary conditions are (see Fig. 1): (a) the phase on the hemisphere at infinity is $\frac{L}{r}$; (b) no current flows through the membrane surface between the pores, i.e. $r_{\theta} = 0$ there; and (c) the phase on the hemisphere of radius r_0 centred at the opening of the i^{th} pore is specified to be $\frac{L}{r_i}$. The choice of surface for the last of the boundary conditions is made for convenience, as it simplifies the resulting mixed boundary value problem whilst enforcing the physical condition of continuity of the phase in the vicinity of the pore opening.

To solve this mixed boundary value problem we appeal to its electrostatics analogy, in which the phase and the superfluid stiffness K_s respectively play the roles of the scalar potential and the permittivity ϵ_0 . To compute the energy at the minimum in terms of the boundary data we apply the divergence theorem to Eq. (1) to obtain the energy in terms of a surface integral:

$$H^L = \frac{K_s}{2} \int_{\partial L} dS \left(\frac{L}{r} \right)^2 - \frac{K_s}{2} \int_L d^3r \left(\frac{L}{r} \right)^2; \quad (3)$$

where the volume (i.e. last) term vanishes because at the minimum-energy configuration $\frac{L}{r}$ obeys $r^2 \nabla^2 \frac{L}{r} = 0$. To simplify the evaluation of the surface integral we make use of the fact that the energy is invariant under global shifts of the potential. Thus, we lower all potentials by $\frac{L}{r}$, which eliminates the contribution from the (left) surface at infinity. What remains are the contributions from the membrane: those from between the pores give zero, owing to the zero-flux boundary condition; those from those from the hemispherical surfaces covering the pores give

$$H^L = \frac{1}{4} \sum_i \left(\frac{L}{r_i} - \frac{L}{r_i} \right) q_i; \quad (4)$$

where, by assumption, the phase $\frac{L}{r}$ takes the constant values $\frac{L}{r_i}$ on the hemispherical surfaces, and the remaining surface integrals have been replaced (via the analogue of Gauss's law) by half of the (analogue of) the charge enclosed. For pore i this charge is $q_i = K_s \int_{\text{hemisphere}} dS \nabla_r \frac{L}{r}$, where the integral is taken over the spherical surface that completes the hemispherical one. Reflecting the problem across the membrane's left surface, we see that we are looking for half of the electrostatic energy of a set of suitably charged metal spheres at potentials $\frac{L}{r_i} - \frac{L}{r}$, and what remains is to determine the charges q_i . To do this, we consider the i^{th} sphere: in the limit $r_0 \rightarrow \infty$ (i.e. ignoring di- and higher-order charge multipoles), the potential on its surface obeys

$$K_s \left(\frac{L}{r_i} - \frac{L}{r} \right) = \sum_j C_{ij}^{-1} q_j; \quad (5a)$$

$$C_{ij}^{-1} = \frac{1}{4} \frac{r_{ij}}{r_0} + \frac{1}{4} \frac{1}{r_{ij}^2}; \quad (5b)$$

where r_{ij} is the distance between the i^{th} and j^{th} pore (sphere) centres, and C_{ij} is the analogue of the capacitance matrix. By solving Eq. (5a) for the q_i 's and eliminating them from Eq. (4), we arrive at the combined energy of the left and right superfluid reservoirs and the superfluid in the pores:

$$E = \frac{K_s}{2} \sum_{ij} \left(\frac{L}{r_i} - \frac{L}{r_j} \right) C_{ij} \left(\frac{L}{r_j} - \frac{L}{r_i} \right) + \sum_i H_i; \quad (6)$$

where we have, without loss of generality, restricted our attention to spatially anti-symmetric states, for which $\frac{L}{R} = -\frac{L}{L}$ and $\frac{R}{r_i} = -\frac{L}{r_i}$.

We complete the description of our model by specifying the single-pore dynamics, and thus the mechanism by which energy is dissipated in the pores. The superfluid velocity \mathbf{v} in a pore of thickness d is determined by the phases at the pore openings: $\mathbf{v} = \frac{1}{m} \nabla \frac{L}{r} \sim 2 \frac{1}{m} \frac{L}{r} \frac{1}{d} = \frac{2}{m} \frac{L}{r} \frac{1}{d}$. Correspondingly the current through the pore is given by

$$I_i = \frac{K_s J}{2} \left(\frac{L}{r_i} - \frac{L}{r_i} \right); \quad (7)$$

When the velocity through the i^{th} pore exceeds its critical value $v_{c,i}$ (or, equivalently, $\frac{L}{r_i} \frac{1}{d}$ exceeds $v_{c,i}$), a vortex line nucleates and moves across the pore, which decreases the phase-difference across the pore by 2π . Thus, immediately after a phase slip, the velocity through the i^{th} pore is decreased by $\frac{2\pi}{m} \frac{1}{d}$, a quantum of superfluid velocity drop for a pore having fixed phases at the openings, i.e. $v_i \rightarrow v_i - \frac{2\pi}{m} \frac{1}{d}$. However, after a very short time, controlled by the speed of sound, the system balances the superflow in the bulk reservoirs and through the various pores. Therefore, after this relaxation process is complete, the actual drop in the superfluid velocity through the i^{th} pore is always less than $\frac{2\pi}{m} \frac{1}{d}$. To find the configuration of the superfluid after a phase slip, we note that the phase-difference along a path from

the left hemispherical surface at infinity through the i^{th} pore to the right hemispherical surface at infinity drops by 2π , whilst the phase-difference along a path through any other pore remains unaffected. In our model, we implement this kind of phase-slip event by sending n_i to $n_i + 1$ (assuming all flow is to the left) and finding a new set of values for all of the L_i 's by minimizing the total energy, Eq. (6).

Not too near T_c the experimentally-observed temperature-dependence of the critical velocity for superflow through a pore is approximately linear [3, 34]: $v_c(T) = v_c(0)(1 - T/T_0)$, where $T_0 \approx 2.5$ K. This T -dependence is most closely reproduced by the thermal nucleation of half-integer vortices mechanism [35]. However, the linear T -dependence does not hold in the temperature regime that we are primarily interested in; instead, the critical velocity is proportional to the superfluid stiffness there [24, 25, 36]:

$$v_c(T) \sim \kappa(T) / K_s(T); \quad (8)$$

where $\kappa(T) \sim \xi_0(1 - T/T_c)^{2.3}$ is the temperature-dependent healing length.

Extrinsic effects are known to reduce critical velocities from the intrinsic values discussed above. We hypothesise that in the Berkeley group's experiments the extrinsic effects originate in atomic-scale roughness of the pore walls, and play a pivotal role in generating critical-velocity variability amongst the pores. This variability is expected to be temperature dependent because only roughness on length-scales longer than $\xi_0(T)$ can substantially perturb the order parameter and thus influence the critical velocities. Hence, at higher temperatures the impact of surface roughness is expected to be weaker and, correspondingly, the distribution of critical velocities is expected to be narrower. Thus, lowering the temperature has the important effective consequence of increasing the effective disorder [37].

Implications of the model | We shall work at fixed (negative) difference in the chemical potential between the reservoirs, so that the control parameter L evolves linearly in time, according to the Josephson-Anderson relation

$$L = \frac{R}{2\pi} t; \quad (9)$$

As L grows, so do the superfluid velocities through the various pores, punctuated at regular intervals by velocity drops associated with the phase-slip processes. As the total energy of the state is periodic in L with period 2π , the total current through the array must be a periodic function of time with the period given by the Josephson frequency $\omega_J = \frac{2eV}{\hbar}$. Due to the randomness of the critical velocities amongst the pores, the velocities in the various pores do not reach their critical values simultaneously. Therefore, the pores having the smaller critical velocities (i.e. the weaker pores) tend to slip first. If the distribution of critical velocities is sufficiently narrow, the array may, as we demonstrate below, suffer an avalanche.

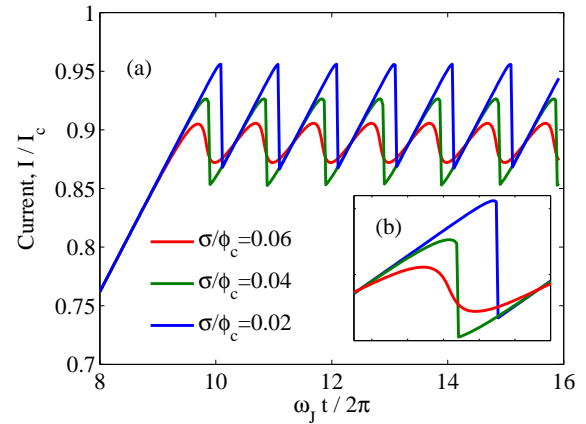


FIG. 3: Time traces of total current through an array of pores as a function of time, at various disorder strengths [38]. The traces were computed at fixed chemical potential difference μ , via our mean-field theory, with Gaussian distributions of critical phase-twists $\phi_{c,i}$ of widths σ and mean $\phi_c = 3$. The corresponding critical current, in the absence of disorder, is given by $I_c = 2K_s J \phi_c$. As the disorder strength is increased, the amplitude of current oscillations decreases. The sharp drops in the current, which correspond to avalanches, disappear for $\sigma/\phi_c > 0.052$.

By an avalanche we mean that when the weaker pores slip, superflow through the neighbouring pores that have yet to slip increases, due to the inter-pore interaction, and this drives them to their own $v_{c,i}$, causing a cascade of phase slips in which an appreciable fraction of pores in the array slip. Experimentally, avalanches are reflected in a periodic series of sharp drops in the total current through the array of pores as a function of time. Time-traces of the total current in the avalanching and non-avalanching regimes are contrasted in Fig. 3.

For arrays having a small number of pores, the quasi-static state of (mechanical) equilibrium may be numerically determined, as the control parameter L evolves parametrically. As a consequence of the long-range nature of the inter-pore couplings, the array dynamics is well approximated by a mean-field theory. We shall describe a numerical approach first, and then the mean-field theory.

The numerics take as input: J , the $v_{c,i}$'s, and the (non-inverted) matrix C_{ij}^{-1} [see Eq. (5b)], which itself depends on r_0 , l , and N . At each time-step, L is incremented, and the new L_i 's are obtained. If the superflow through any pore is found to now exceed its critical velocity, that pore phase-slips (i.e. its value of n_i is incremented by plus unity); next, the various L_i 's are recomputed using the new set of n_i 's, and the program goes back to recheck if any other pore now exceeds its critical velocity. This continues until no new phase-slips are found to occur, at which point the control parameter is incremented and the procedure is repeated.

Next, we construct a mean-field theory. We assert that

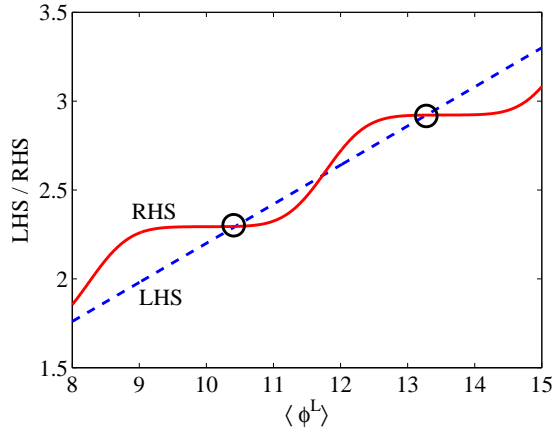


FIG. 4: Left- and right-hand sides of the averaged form of Eq. (10). The circles indicate the two main solutions: as the control-phase is increased, the RHS curve moves up and to the left, such that there is a discontinuous jump from one solution to the other corresponding to an avalanche.

$$\ln i(h^L i) = \sum_k \sum_{c=0}^{Z-1} d_c Q(c) \left[\frac{A^L + B h^L i}{C + 2J} - \frac{k C}{C + 2J} \right]; \quad (11)$$

where $Q(c)$ is the probability distribution of half-critical phase twists in the pores $c = \text{dim } v_c \sim \sim$. The averaged form of Eq. 10 can be solved graphically, by plotting the left- and right-hand sides as functions of $h^L i$; see Fig. 4. It is evident from this graphical approach that whenever the maximum slope of the right-hand side, $2J \ln i = \partial h^L i$ fails to exceed the slope of the left-hand side, $(A + 2J)h^L i$, the self-consistency condition yields a unique solution for the average phase $h^L i$, and that this phase evolves continuously with the (increasing) control-phase ϕ^L . This corresponds to the non-avalanching regime. By contrast, whenever the maximum slope of the right-hand side does exceed the slope of the left-hand side, the self-consistency condition no longer yields a unique solution for $h^L i$. Instead, as the control-phase increases, the continuous evolution of $h^L i$ is punctuated by jumps, which occur when pairs of solutions merge and disappear. These jumps reflect avalanching behaviour, and we refer to this as the avalanching regime.

One can use this mean-field theory to construct a phase diagram that demarcates avalanching and non-avalanching regimes, for any choice of disorder distribution Q . For the case of a top-hat distribution of critical phase-twists, a simple inequality defines the avalanching regime:

$$w > w_c = \frac{2JB}{(A + 2J)(C + 2J)}; \quad (12)$$

the control-phase-difference is monotonically increasing in time, so that phase differences $\phi_i^L - \phi_i^R$ are always increasing and the superflow in the pores undergoes only n_i -increasing phase slips. Then we may proceed by selecting an arbitrary pore i , and minimizing the energy (6) with respect to ϕ_i^L ; by replacing the $\phi_{j(\neq i)}^L$'s by their mean-field value $h^L i$ we obtain an equation for the phase at the i^{th} pore:

$$\phi_i^L (C + 2J) - B h^L i = A^L + 2J n_i; \quad (10)$$

where $A = \sum_j C_{ij}$, $B = C_{ii} - A$, and $C = G_i$ [39]. (The necessary inversion of C_{ij}^{-1} can readily be accomplished either analytically, by transforming to Fourier space, or numerically.) By averaging the left- and right-hand sides of this equation over sites, we arrive at a self-consistency condition on $h^L i$. Next, by assuming self-averaging with respect to the disorder in the critical velocities, we may replace the average over sites by an average over disorder. This procedure amounts to replacing, in the above condition, ϕ_i^L by $h^L i$ and n_i by

where w is the width of the top hat, and w_c is its critical value; such a phase boundary is exemplified in Fig. 2. In experiments, one can explore this phase diagram by tuning the temperature, which, as we have hypothesised above, effectively tunes the strength of the disorder.

Thermal fluctuations of the phases wash out the disorder-driven phase transition if they exceed the width of the disorder distribution. To avoid this, the temperature has to be smaller than the energy cost of winding the phase of a single pore by the critical disorder width, i.e. $k_B T < K_s(T) C w_c^2 = 2$. We estimate that this inequality is satisfied provided that T is not too close to the point, i.e. $T < T_c \approx 3 \text{ mK}$ in the setting of Ref. [1]. Furthermore, we have assumed that the current-phase relation is linear, which is true provided that $T < T_c \approx 5 \text{ mK}$, as was measured for a similar setup in Ref. [14].

To test the results of the mean-field theory, we have compared them to results from a numerical investigation performed on a finite, periodic lattice [39]. For various widths of the disorder distribution (which we have taken to be Gaussian), the fractions of pores that have phase-slipped, as a function of control-parameter, are shown in the inset of Fig. 2. As predicted by the mean-field theory, avalanches occur when the distribution of critical velocities is narrow but not when it is broad. At a critical strength of the disorder, which separates these two regimes, the discontinuity in the mean-field fraction of slipped pores just vanishes. Moreover, at this critical

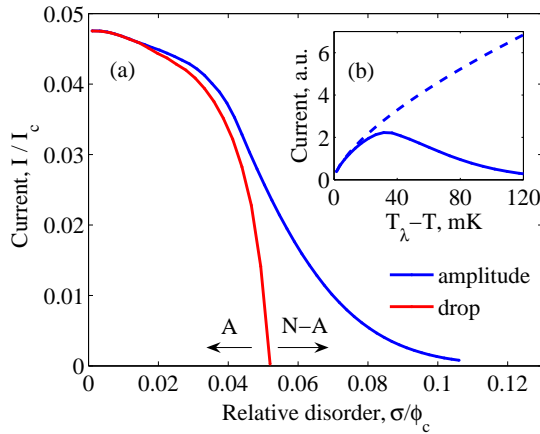


FIG. 5: Amplitude of the oscillations of the current I , and drop in the current caused by an avalanche, as functions of the disorder strength. A and N-A indicate the avalanching and non-avalanching regimes, respectively. Inset: Solid line: amplitude of the current oscillations as a function of temperature, using the disorder model described in the text. Dashed line: expected amplitude in the absence of disorder.

disorder there are always values of the control phase at which the response of the system diverges. The mean-field and numerical results appear to agree with one another rather well, as one can see from Fig. 2, at least in the vicinity of the critical point.

The two main results of our Paper are summarised in Fig. 5. The blue curve shows the dependence of the amplitude of the current oscillation I (i.e. half the distance between smallest and largest current during a single period in Fig. 3) on the disorder strength. As the disorder becomes stronger, the phase-slips in the various pores become more asynchronous, and the oscillations in the current gradually disappear. The red curve shows the dependence of the current drop caused by an avalanche (i.e. the height of the vertical drop in current in Fig. 3) on the disorder strength. The current-drop plays the role of an order-parameter in a second-order phase transition tuned by the disorder strength. As the disorder becomes stronger, the order-parameter decreases, becoming zero at the critical disorder strength corresponding to the transition from the avalanching to the non-avalanching regime (i.e. $c_c = 0.052 c_0$).

Comparison with experiments | In their experiments [1], the Berkeley group have measured the amplitude of the "whistle" (i.e. the amplitude of the current oscillations I) as a function of temperature at a fixed chemical potential difference. The experiments found that at T_c there are no oscillations of the current. As the temperature is lowered below T_c , I first increases, and then gradually decreases. To obtain the behaviour of I as a function of T we extend the model for the critical veloc-

ity, Eq. (8), to include disorder, by assuming that

$$v_{c,i}(T) \sim \frac{\tilde{v}}{m(\langle T \rangle + x_i)}; \quad (13)$$

where x_i is the temperature-independent characteristic scale of the surface roughness in the i^{th} pore, which we take to have a Gaussian distribution [40]. For $T_c - T > 5 \text{ mK}$, we can compare the results of our modelling to those of the experiments. The general features are reproduced: the initial increase in I is associated with an increase in the superfluid fraction; the gradual decrease at lower temperatures is due to the loss of synchronicity amongst the pores, which is caused by the effective increase in the strength of disorder. To demonstrate these features, we plot the amplitude of current oscillations as a function of temperature; see the inset in Fig. 5, for which we have set $x = 4 \text{ nm}$.

We also note that the general features of the current-vs.-time traces, Fig. 3, are similar to those of the type III experiments described in Ref. [1]. In both, as the temperature is lowered (i.e. the disorder is increased), the avalanche gradually disappears, and then so do the oscillations in the current.

Concluding remarks | Motivated by recent experiments performed by the Berkeley group on superflow through nanopore arrays [1], we have developed a model to describe phase-slip dynamics of such systems. The main features of our model are effective inter-pore couplings, mediated through the bulk superfluid, as well as randomness in the critical velocities of the pores, the latter being effectively controlled through the temperature.

Within our model, we find that the competition between (a) site-disorder in the critical velocities and (b) effective inter-pore coupling leads to the emergence of rich collective dynamics, including a transition between avalanching and non-avalanching regimes of the phase-slip dynamics. We identify a line of critical disorder-strengths in the phase diagram, at which there is a divergent susceptibility, in the sense that near to this line small changes in the control parameter can lead to large changes in the fraction of phase-slipped pores.

Our model reproduces the key physical features of the Berkeley group's experiments [1], including a high-temperature synchronous regime, a low-temperature asynchronous regime, and a transition between the two. We therefore feel that the model captures the essential physics explored in these experiments.

In a forthcoming paper we shall extend our approach in order to address the transition from the Josephson regime to the avalanching phase-slippage regime described here, by including thermal fluctuations together with a generalised description of pore energies that is valid in both regimes.

Acknowledgements | It is a pleasure for us to express our gratitude to Richard Packard for introducing us to the subject-matter explored in this Paper, for describing his group's experiments to us, and for furnishing us with data of theirs, prior to publication. We are similarly

grateful to his group members Yuki Sato and Aditya Joshi. We thank Karim Dahmen for guiding us through the literature on analogous physical systems, and Tzu-Chieh Wei and Smitha Vishveshwara for useful discussions. This work was supported by the U.S. Department

of Energy, Division of Materials Sciences under Award No. DEFG 02-96ER 45434, through the Frederick Seitz Materials Research Laboratory at the University of Illinois at Urbana-Champaign.

-
- [1] Sato, Y., Hoskinson, E. & Packard, R.E. Transition from synchronous to asynchronous superfluid phase slippage in an aperture array. *cond-mat/0605660*.
- [2] Tinkham, M. Introduction to Superconductivity, (McGraw-Hill, New York, 1996).
- [3] Tilley, D.R. and Tilley, J. Superfluidity and Superconductivity, 3rd ed. (Hilger, New York, 1990).
- [4] Dalfovo, F., Giorgini, S., Pittaevskii, L.P., & Stringari, S. Theory of Bose-Einstein condensation in trapped gases. *Rev. Mod. Phys.* 71, 463-512 (1999).
- [5] Kim, E. & Chan, M.H.W. Probable observation of a supersolid helium phase. *Nature* 427, 225-227 (2004).
- [6] Josephson, B.D. Possible new effects in superconductive tunnelling. *Phys. Lett.* 1, 251-253 (1962).
- [7] Rowell, J.M. Magnetic Field Dependence of the Josephson Tunnel Current. *Phys. Rev. Lett.* 11, 200-202 (1963).
- [8] Giaever, I. Detection of the ac Josephson Effect. *Phys. Rev. Lett.* 14, 904-906 (1965).
- [9] Albiez, M. et al. Direct Observation of Tunneling and Nonlinear Self-Trapping in a Single Bosonic Josephson Junction. *Phys. Rev. Lett.* 95, 010402 (2005).
- [10] Avenel, O. & Varoquaux, E. Josephson effect and quantum phase slippage in superfluids. *Phys. Rev. Lett.* 60, 416-419 (1988).
- [11] Backhaus, S., Pereverzev, S.V., Loshak, A., Davis, J.C. & Packard, R.E. Direct Measurement of the Current-Phase Relation of a Superfluid $^3\text{He-B}$ Weak Link. *Science* 278, 1435-1438 (1997).
- [12] Davis, J.C. & Packard, R.E. Superfluid ^3He Josephson weak links. *Rev. Mod. Phys.* 74, 741-773 (2002).
- [13] Sukhatme, K., Mukharsky, Yu., Chui, T. & Pearson, D. Observation of the ideal Josephson effect in superfluid ^4He . *Nature* 411, 280-283 (2001).
- [14] Hoskinson, E., Sato, Y., Hahn, I. & Packard, R.E. Transition from phase slips to the Josephson effect in a superfluid ^4He weak link. *Nature Physics* 2, 23-26 (2006).
- [15] Anderson, P.W. Basic Notions of Condensed Matter Physics (Benjamin/Cummings Publ., Menlo Park, 1984).
- [16] Clarke J. & Braginski A.I. (editors) The SQUID Handbook: Applications of SQUIDS and SQUID Systems, Volume II (John Wiley & Sons, 2006).
- [17] Mukharsky, Yu., Avenel O. & Varoquaux, E. Rotation measurements with a superfluid ^3He gyrometer. *Physica B* 284-288 287-288 (2000).
- [18] Simmonds, R.W., Marchenkov, A., Hoskinson, E., Davis, J.C. & Packard, R.E. Quantum interference of superfluid ^3He . *Nature* 412, 55-58 (2001).
- [19] Zimmerman, W. In Proceedings of the Fifth Oregon Conference on Liquid Helium, A Report from the Department of Physics, University of Oregon, 1987, p. 118.
- [20] Chui, T., Holmes, W. & Penanen, K. Fluctuations of the Phase Difference across an Array of Josephson Junctions in Superfluid ^4He near the Lambda Transition. *Phys. Rev. Lett.* 90, 085301 (2003).
- [21] For ^4He , thermal fluctuations strongly suppress the DC Josephson effect in a single pore [9, 20]. To overcome this difficulty, experiments are conducted using arrays of pores; see, e.g., Ref. [13].
- [22] R.P. Feynman, in Progress in Low Temperature Physics, edited by C. J. Gorter (North-Holland, Amsterdam, 1955), Vol. 1, Chap. 2.
- [23] Anderson, P.W. Considerations on the flow of superfluid Helium. *Rev. Mod. Phys.* 38, 298-310 (1966).
- [24] Iordanskii, S.V. Vortex ring formation in a superfluid. *Zh. Eksp. Teor. Fiz.* 48, 708-714 (1965) [*Sov. Phys. JETP* 21 467-471 (1965)].
- [25] Langer, J.S. & Fisher, M.E. Intrinsic critical velocity of a superfluid. *Phys. Rev. Lett.* 19 560-563 (1967).
- [26] Hoskinson, E., Packard, R.E. & Haard, T.M. Quantum whistling in superfluid helium 4. *Nature* 433, 376-376 (2005).
- [27] Hopkins, D.S., Pekker, D., Goldbart, P.M. & Bezryadin, A. Quantum interference device made by DNA templating of superconducting nanowires. *Science* 308, 1762-1765 (2005).
- [28] Burridge R. & Knopoff, L. Model and theoretical seismicity. *Bull. Seismol. Soc. Am.* 57, 341-371 (1967).
- [29] Sethna, J.P. et al. Hysteresis and hierarchies: Dynamics of disorder-driven first-order phase transformations. *Phys. Rev. Lett.* 70, 3347-3350 (1993).
- [30] for a review, see, Fisher, D.S., Collective transport in random media: from superconductors to earthquakes. *Phys. Repts.* 301, 113-150 (1998).
- [31] also see, Marchetti, M.C. Depinning and plasticity of driven disordered lattices. *cond-mat/0503660* and references therein.
- [32] In particular, one can make evident the kinship between the present superfluid model and the elastic model for CDW depinning (without topological excitations) by exchanging control via the chemical potential difference between the reservoirs for control via the supercurrent, which then plays the role of the CDW driving force.
- [33] Beecken, B.P. & Zimmerman, W. Jr., Variation of the critical order-parameter phase difference with temperature from 0.4 to 1.9 K in the flow of superfluid ^4He through a tiny orifice. *Phys. Rev. B* 35, 1630-1635 (1987).
- [34] Avenel, O., Ihas, G.G. & Varoquaux, E. The nucleation of vortices in superfluid ^4He : answers and questions. *J. Low Temp. Phys.* 93, 1031-1057 (1993).
- [35] Volovik G.E. Quantum-mechanical formation of vortices in a superfluid. *ZhETF Pis. Red.* 15, 116-120 (1972) [*JETP Lett.* 15, 81-83 (1972)].
- [36] Hess, G.B. Critical velocities in superfluid Helium flow through 10 μm -diameter pinholes. *Phys. Rev. Lett.* 27, 977-979 (1971).
- [37] Similar ideas have been suggested by Y. Sato and co-workers (private communication (2006)).
- [38] $A = 0.02 \text{ m}$; $B = 0.16 \text{ m}$; $C = 0.18 \text{ m}$; $J = 0.05 \text{ m}$.

[39] We wish to eliminate effects arising from edges of the array of pores. We do this by measuring distances between pairs of sites, allowing paths to wrap around the edges and picking the shortest one. This renders the problem translationally invariant. In particular, A , B , and C_{ij} are

then independent of any pore index.
[40] The Gaussian distribution is suitably cut-off and renormalized to avoid negative or very large critical velocities.